Compositional Power Flow for Networked Microgrids

Yan Li, *Member, IEEE,* Peng Zhang, *Senior Member, IEEE,* Chongqing Kang, *Fellow, IEEE*

***Abstract*—In this letter, a compositional power flow (ComPF) is devised for networked microgrids to take into account power sharing and voltage regulation between microgrids while preserving data privacy of each microgrid. The main contributions of ComPF include: 1) devise an advanced-droop-control-based power flow to incorporate distributed energy resources (DERs) and load droops within microgrids; 2) establish an adaptive-secondary-control-based compositional power flow scheme to account for power sharing and voltage regulation between microgrids. As an inherently distributed method, ComPF supports plug-and-play of microgrids and preserves customer privacy.**

***Index Terms*—ComPF, Advanced Droop Control, Adaptive Secondary Control, Privacy Preserving.**

I. INTRODUCTION

NETWORKED microgrids (NMs) is a new paradigm [1], [2], [3] which unlocks the potentials of microgrids such as enabling the power exchange among microgrids [4], the pooling of generating capacities in microgrid clusters for supporting critical loads, and even quickly blackstarting main grid after major blackout [5]. An indispensable function for planning and operation of NMs is power flow calculation which, however, remains an open challenge.

The major bottlenecks for NM power flow include: 1) an islanded microgrid no longer has a swing bus; rather, both distributed energy resources (DERs) and loads follow droop characteristics, which has not been fully addressed by the state of the art methods [6], [7]. 2) NMs are designed to support plug-and-play of neighboring microgrids and achieve voltage restoration and power sharing through secondary control, which cannot be solved by existing centralized power flow analysis methods [8]. Moreover, existing methods require full access to individual microgrid data, while few microgrid owners would permit disclosure of their privacy [9], [10].

In this letter, to address the inherent difficulties in NM power flow, we contribute a novel compositional power flow (ComPF) method which fully supports plug-and-play of microgrids, incorporates DER/load droops within a microgrid, takes into account the voltage regulation and power sharing for NMs, and protects data privacy via limited data exchange.

II. COMPOSITIONAL POWER FLOW

To tackle the NM power flow, a compositional scheme is introduced, originally invoked in the formal methods community [11], [12], that provides network-level solutions from power flow solutions of individual microgrids and their interconnections. Specifically, ComPF is a framework that integrates an advanced-droop-control-based power flow (ADPF) for islanded microgrids and adaptive-secondary-control-based power flow (ASPF) for NMs, as shown in Fig. 1.

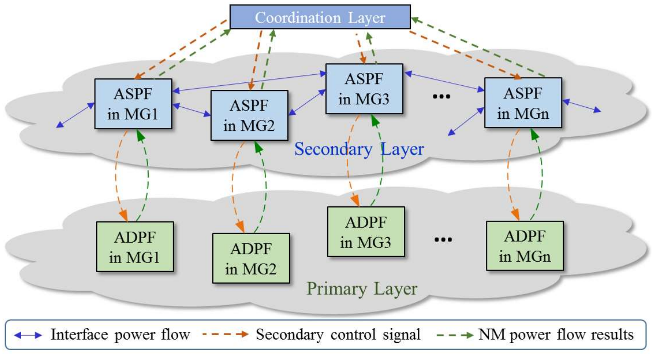

Fig. 1. Algorithmic framework for ComPF.

A. ADPF for Islanded Microgrids

When a microgrid operates in islanded mode and cannot fully cover its load, the P/F-Q/V droop strategy is usually adopted in DERs and loads as shown in Fig. 2.

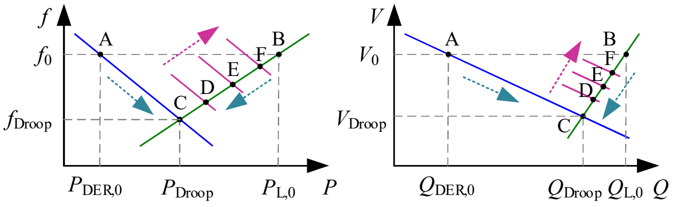

Fig. 2. Schematics of ADPF and ASPF.

Assume in Microgrid i, DERs initially operate at point A, whereas the load demand reaches point B. ADPF will then adjust both DER generation and load demand in each iteration according to (1) and (2), and eventually Microgrid i will reach an equilibrium at point C.

$$\Delta \mathbf{P_i} = (f^r - f)/\mathbf{m_{P,i}}, \tag{1}$$

$$\Delta \mathbf{Q_i} = (\mathbf{V_i^r} - \mathbf{V_i})/\mathbf{m_{Q,i}}, \tag{2}$$

where $\mathbf{m_{P,i}}$ and $\mathbf{m_{Q,i}}$ are the droop coefficient vectors of P/F and Q/V; f^r and $\mathbf{V_i^r}$ are the references of frequency and voltage vector; f and $\mathbf{V_i}$ are the actual values of frequency and voltage vector in each iteration. Here f is a global variable, and $\mathbf{V_i}$ is a local vector only available for local buses in Microgrid i without assuming a communication network.

This work was supported in part by the National Science Foundation under Grants ECCS-1611095, CNS-1647209 and ECCS-1831811.

Y. Li and P. Zhang are with the Department of Electrical and Computer Engineering, University of Connecticut, Storrs, CT 06269-4157, USA (e-mails: yan.7.li@uconn.edu, peng.zhang@uconn.edu).

C. Kang is with the Department of Electrical Engineering, Tsinghua University, Beijing 100084, China (e-mail: cqkang@tsinghua.edu.cn).

B. ASPF for Networked Microgrids

On top of ADPF, ASPF accounts for coordination operations between microgrids. Define the power exchanges between Microgrids i and j as the vector $\mathbf{S_{i,j}} = \mathbf{P_{i,j}} + j\mathbf{Q_{i,j}}$, then the voltages of each microgrid can be updated as:

$$\mathbf{V_i} = \mathbf{V_i^r} - \mathbf{BCBV_i} \cdot \mathbf{BIBC_i} \cdot \{(\mathbf{S_i} + \mathbf{S_{i,j}})/\mathbf{V_i}\}^*, \quad (3)$$

where $\mathbf{BCBV_i}$ and $\mathbf{BIBC_i}$ are the Branch Current to Bus Voltage matrix and Bus Injection to Branch Current matrix pertaining to Microgrid i [8], and $\mathbf{S_i}$ is the load vector of Microgrids i. Depending on NM's operating strategy, $\mathbf{S_{i,j}}$ may be updated in any of the following ways:

1) Voltage Control Mode: Here the objective is to regulate the voltages at leading DER bus in each microgrid (see point B in Fig. 2). Simulation studies show that, if power exchanges and the leading DER voltage are treated independently, ComPF is hard to converge. To resolve this issue, power exchange are associated with secondary control as follows:

$$\mathbf{P_{i,j}} = \mathbf{P_{i,j}^P} - \alpha_i \cdot \mathbf{P_{base,i}} \cdot real(\mathbf{V_{DER,i}^r} - \mathbf{V_{DER,i}}), \quad (4)$$

$$\mathbf{Q_{i,j}} = \mathbf{Q_{i,j}^P} + \beta_i \cdot \mathbf{Q_{base,i}} \cdot imag(\mathbf{V_{DER,i}^r} - \mathbf{V_{DER,i}}), (5)$$

where $\mathbf{P_{i,j}^P}$ and $\mathbf{Q_{i,j}^P}$ are the active and reactive power exchanges from the previous iteration, $\mathbf{P_{base,i}}$ and $\mathbf{Q_{base,i}}$ are the base values (usually set as the maximum power of Microgrid i) that scale voltage changes making them comparable to power changes, α_i and β_i are step sizes, $\mathbf{V_{DER,i}^r}$ and $\mathbf{V_{DER,i}}$ are the reference values and actual values of leading DER voltage, $real(\cdot)$ and $imag(\cdot)$ are functions to get the real and imaginary parts. (4) and (5) are set based on the fact that active power is strongly correlated to the real part of voltage whereas reactive power is correlated to the imaginary one.

2) Power Dispatch Mode: Here the objective is to control power exchanges across the interface when a microgrid with power deficit is supported by its neighbors. Since the power exchanges among microgrids can be determined by the voltages across their interfaces, it is equivalent to control the voltages at the interface buses. Once the power exchange $\mathbf{S_{i,j}}$ are scheduled in the networked microgrid coordination layer (or an energy management system if it exists), (3) can be used to solve power flow in each microgrid. Specifically, a DER bus is usually selected as the adaptive swing bus [8], and its voltage is updated based on the voltage mismatches of the interface buses as follows:

$$V_{i,s} = V_{i,s}^r + \{\mathbf{BCBV_i} \cdot \mathbf{BIBC_i} \cdot \{(\mathbf{S_i} + \mathbf{S_{i,j}})/\mathbf{V_i}\}^*\}_k, \quad (6)$$

where $V_{i,s}$ and $V_{i,s}^r$ are the voltages of the adaptive swing bus and its corresponding reference value for Microgrid i, $\{\mathbf{BCBV_i} \cdot \mathbf{BIBC_i} \cdot \{(\mathbf{S_i} + \mathbf{S_{i,j}})/\mathbf{V_i}\}^*\}_k$ is the voltage deviation at the interface bus k. Then $V_{i,s}$ will be used to update the voltage of other buses in Microgrid i via (3).

Under the voltage update mechanism in (6), the interface bus voltages can be controlled at the desired values to achieve the scheduled power exchanges.

The aforementioned ASPF results in an adaptive and secure architecture because:

- Both control modes can be implemented within one architecture, triggered by different control demands.
- Only limited data, i.e., DER voltages and power exchanges in the voltage control mode and power exchanges in the power dispatch mode, need to be sent to the coordination layer to calculate the power exchanges.

C. ComPF Algorithm

The overall ComPF algorithm follows a triple loop process. The *primary loop* is to solve the power flow problem based on the updated power of DERs and loads via the *secondary loop*. The *tertiary loop* is to update the power exchanges through NM interfaces. ComPF is described in *Algorithm 1.*

Currently, the direct backward/forward sweep [6] is embedded in Algorithm 1 in view of the fact that most microgrids operate with a tree structure. Nevertheless, the principle of ComPF is generic because other techniques including modified Newton, implicit Z_{bus} Gauss, current injection, can be likewise adopted under this framework.

Algorithm 1: ComPF Algorithm

```
Initialize $\mathbf{BCBV_i}$, $\mathbf{BIBC_i}$, $\mathbf{P_i^0}$, $\mathbf{Q_i^0}$, $\mathbf{V_i}$, $\mathbf{V_i^r}$, $f$, $f^r$
repeat
    Update $\mathbf{P_{i,j}}$, $\mathbf{Q_{i,j}}$    Eq. (4/5) or given value
    repeat
        Update $\Delta\mathbf{P_i}$, $\Delta\mathbf{Q_i}$    Eq. (1/2)
        repeat
            Update $\mathbf{V_i}$    Eq. (3/6)
        until $\mathbf{V_i}$ is constant;
        Update $\mathbf{V_i}$, $f$
    until $V_{i,s}$ and $f$ are constant;
    Update $\mathbf{V_{DER,i}}$
until $\mathbf{V_{DER,i}}$ or $\mathbf{P_{i,j}}$, $\mathbf{Q_{i,j}}$ is constant;
```

III. CASE STUDY

The effectiveness of ComPF is validated on a 69-bus NM system consisting of three microgrids (see Fig. 3). The base voltage of the test NM system is 12.66 kV, base power is $5,000$ kVA. More details of the test system can be found in [13]. All of the six DERs in Fig. 3 are dispatchable. ComPF is evaluated in four cases in order to better evaluate the efficacy of ComPF. *Case 1* verifies the correctness of ADPF by operating three islanded but unconnected microgrids through droop control only . *Case 2* subsequently interconnects three microgrids by closing the two tie switches and observes the NM behaviors during natural power exchanges. Based on *Case 2*, *Case 3* and *Case 4* are constructed by increasing both active power and reactive power of Load 61 in Microgrid 2 by 50%. Specifically, *Case 3* verifies the efficacy of ComPF under the voltage control mode, while *Case 4* focuses on verifying ComPF under the power dispatch mode.

Case1: ADPF Calculation: The droop coefficients of loads at buses $\{28, 45, 46, 49, 61, 64, 11, 12\}$ are set to the same value 10.0, because it is assumed that these loads have the same characteristics. Here the P/F and Q/V use the same droop coefficients. The rating of DERs at buses $\{1, 29, 50, 61, 16, 27\}$ and their droop coefficients are summarized in

This article has been accepted for publication in a future issue of this journal, but has not been fully edited. Content may change prior to final publication. Citation information: DOI 10.1109/JPETS.2019.2897780, IEEE Power and Energy Technology Systems Journal

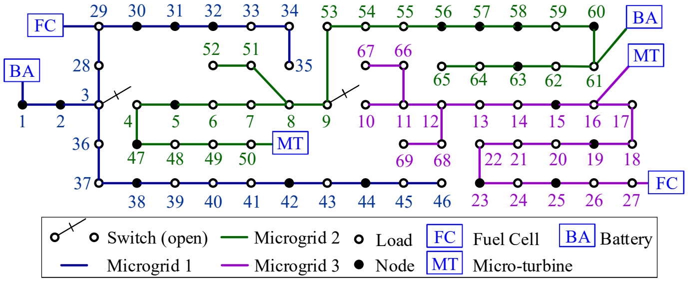

Fig. 3. Test NM system.

Table I, from which it can be seen that droop coefficients are inversely proportional to the DER rated power. Under droop control, the frequencies of the three microgrids are stabilized at 59.5895Hz, 59.6569Hz, 59.8111Hz, respectively.

TABLE I
RATED POWER AND DROOP COEFFICIENTS OF DERS

DER Bus Number	1	29	50	61	16	27
Rated Power(kW)	$2,160$	$1,440$	$2,700$	$1,800$	$2,160$	$1,080$
Droop Coefficients	1.0	1.5	0.8	1.2	1.0	2.0

Case2: Free Interconnection of Microgrids: This case emulates the microgrid synchronization process where the three microgrids are interconnected after the microgrid frequencies and interface bus voltages are regulated to nominal values. *Case3: Networking Microgrids in Voltage Control Mode*: The objective is to adjust DER power outputs to maintain the DER terminal voltages at 1.01 p.u., meanwhile covering the loads. The stopping tolerance for each microgrid is set as 10^{-6} p.u., whereas that for their interfaces is set as 10^{-3} p.u..

TABLE II
DER/LOAD ADJUSTMENTS AND DROOPS CALCULATED WITH ADPF RESULTS FOR MICROGRID I (STOPPING TOLERANCE: 10^{-6} P.U.)

	Initial Values (kVA)	ADPF Values (kVA)	$\Delta f/\Delta \mathbf{P_i}$	$\Delta \mathbf{V_i}/\Delta \mathbf{Q_i}$
DER1	$150.00 + j150.00$	$184.21 + j166.70$	0.9999	1.0000
DER29	$60.00 + j10.00$	$82.81 + j21.21$	1.4997	1.5005
Load28	$26.00 + j18.60$	$22.58 + j16.93$	10.0027	10.0185
Load45	$39.22 + j26.30$	$35.80 + j23.92$	10.0027	10.0076
Load46	$39.22 + j26.30$	$35.80 + j23.92$	10.0027	10.0084

Case4: Networking Microgrids in Power Dispatch Mode: The objective here is to adjust DER power outputs to actively dispatch power among microgrids. Specifically, DER outputs in Microgrid 2 are capped at the same level as in *Case2* as the DERs reach their capacity limits, whereas Microgrids 1 and 3 provide the agreed power exports (in this case equally shared) to offset the load change in Microgrid 2.

Note that, to better illustrate the convergence process, the voltage differences between non-swing buses and the adaptive swing bus in Microgrid i, $\mathbf{r}_i$, is scaled up by $\| \mathbf{c}_i \|_2 = -10/ln(\| \mathbf{r}_i \|_2)$, where $\| \cdot \|_2$ is the l_2-norm [14], [15].

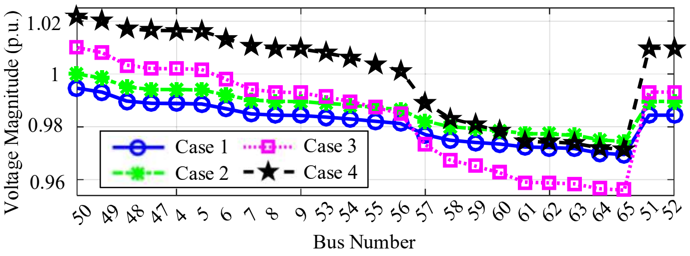

Fig. 4. Voltage magnitude in Microgrid 2.

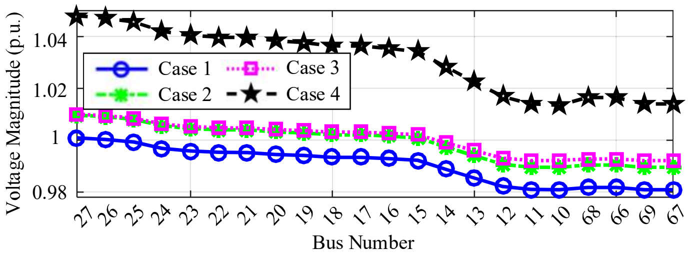

Fig. 5. Voltage magnitude in Microgrid 3.

A few insights can be obtained by observing the test results:

- The droop coefficients inversely calculated from the ADPF results (see Table II) are identical to the preset droop values, which proves the correctness of ADPF.
- *Case3* indicates that, for NMs operating in the voltage control mode, all DER voltages are controlled as prescheduled. However, as shown in Figs. 4 and 5, the voltage profile of Microgrid 2 is inferior to that in *Case2* due to the excessive load and the lack of scheduled power assistance from neighboring microgrdis.
- *Case4* shows that power exchanges are correctly dispatched between microgrids to fix the power deficit in Microgrid 2, which verifies the efficacy of ComPF. DER outputs in different cases are compared in Figs. 6 and 7.
- The iterations for *Case3* including those at the microgrid interfaces and within microgrids are illustrated in Fig. 8, showing a satisfactory convergence performance.
- In summary, ComPF solves efficiently with reduced data exposures and enhanced privacy.

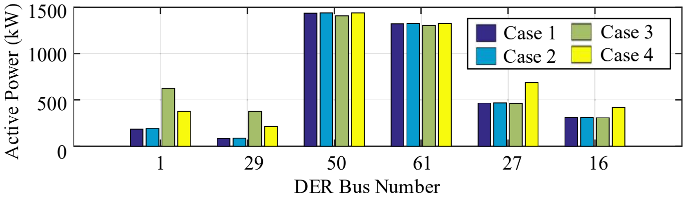

Fig. 6. Active power outputs of DERs.

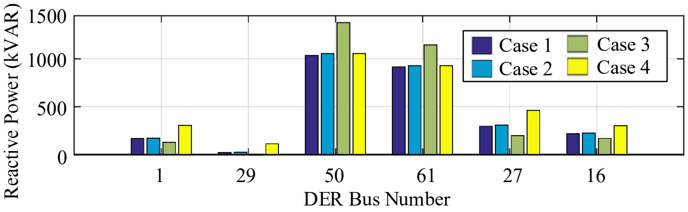

Fig. 7. Reactive power outputs of DERs.

This article has been accepted for publication in a future issue of this journal, but has not been fully edited. Content may change prior to final publication. Citation information: DOI 10.1109/JPETS.2019.2897780, IEEE Power and Energy Technology Systems Journal

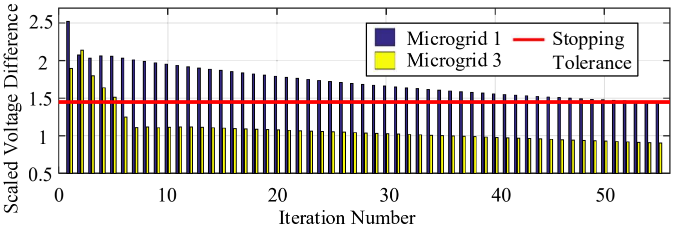

(a) Scaled voltage differences on the interfaces during iterations

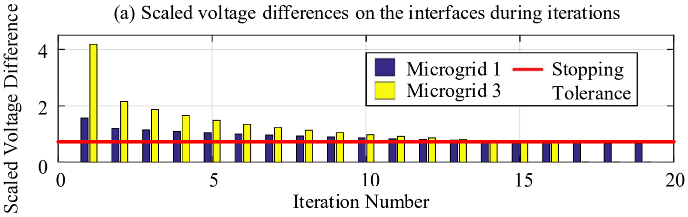

(b) Scaled voltage differences at iteration 40 in (a)

Fig. 8. Convergence process in Case3.

IV. CONCLUSION

A privacy-preserving ComPF is devised by successfully integrating advanced droop control, voltage control mode, and power dispatch mode in networked microgrids. Test results on a typical networked microgrid system validate the efficacy and efficiency of ComPF, which verifies the potential of ComPF as a powerful tool for NM planning, design, and operation.

REFERENCES

[1] Y. Li, P. Zhang, and P. B. Luh, "Formal analysis of networked microgrids dynamics," *IEEE Transactions on Power Systems*, vol. 33, no. 3, pp. 3418–3427, 2018.
[2] Y. Li, P. Zhang, and M. Yue, "Networked microgrid stability through distributed formal analysis," *Applied Energy*, vol. 228, pp. 279–288, 2018.
[3] Y. Li, Y. Qin, P. Zhang, and A. Herzberg, "Sdn-enabled cyber-physical security in networked microgrids," *IEEE Transactions on Sustainable Energy*, 2018.
[4] A. Kahrobaeian and Y. A.-R. I. Mohamed, "Networked-based hybrid distributed power sharing and control for islanded microgrid systems," *IEEE Transactions on Power Electronics*, vol. 30, no. 2, pp. 603–617, 2015.
[5] Y. Zhao, Z. Lin, Y. Ding, Y. Liu, L. Sun, and Y. Yan, "A model predictive control based generator start-up optimization strategy for restoration with microgrids as black-start resources," *IEEE Transactions on Power Systems*, vol. 33, no. 6, pp. 7189–7203, 2018.
[6] G. Díaz, J. Gómez-Aleixandre, and J. Coto, "Direct backward/forward sweep algorithm for solving load power flows in AC droop-regulated microgrids," *IEEE Transactions on Smart Grid*, vol. 7, no. 5, pp. 2208–2217, 2016.
[7] F. Hameed, M. Al Hosani, and H. Zeineldin, "A modified backward/forward sweep load flow method for islanded radial microgrids," *IEEE Transactions on Smart Grid*, 2017.
[8] L. Ren and P. Zhang, "Generalized microgrid power flow," *IEEE Transactions on Smart Grid*, 2018.
[9] S. A. Salinas and P. Li, "Privacy-preserving energy theft detection in microgrids: A state estimation approach," *IEEE Transactions on Power Systems*, vol. 31, no. 2, pp. 883–894, 2016.
[10] K. G. Boroojeni, M. H. Amini, and S. S. Iyengar, *Smart grids: security and privacy issues*. Springer, 2017.
[11] M. Rungger and M. Zamani, "Compositional construction of approximate abstractions of interconnected control systems," *IEEE Transactions on Control of Network Systems*, vol. 5, no. 1, pp. 116–127, 2018.
[12] S. W. Smith, P. Nilsson, and N. Ozay, "Interdependence quantification for compositional control synthesis with an application in vehicle safety systems," in *Decision and Control (CDC), 2016 IEEE 55th Conference on*. IEEE, 2016, pp. 5700–5707.
[13] J. Savier and D. Das, "Impact of network reconfiguration on loss allocation of radial distribution systems," *IEEE Transactions on Power Delivery*, vol. 22, no. 4, pp. 2473–2480, 2007.
[14] Y. Li, P. Zhang, M. Althoff, and M. Yue, "Distributed formal analysis for power networks with deep integration of distributed energy resources," *IEEE Transactions on Power Systems*, 2018.
[15] T. Hofmann, "Probabilistic latent semantic indexing," in *ACM SIGIR Forum*, vol. 51, no. 2. ACM, 2017, pp. 211–218.

Yan Li (M'18) received the B. Sc. and M. Sc. degrees in Electrical Engineering from Tianjin University, Tianjin, China, in 2008 and 2010, and the Ph.D. degree in Electrical Engineering at University of Connecticut, Storrs, CT, USA, in 2018. Her research interests include microgrids and networked microgrids, formal analysis, power system stability and control, software defined networking, and cyber-physical security.

Peng Zhang (M'07−SM'10) received the Ph.D. degree in electrical engineering from the University of British Columbia, Vancouver, BC, Canada, in 2009. He is the Centennial Chair Professor, and Associate Professor of Electrical Engineering at the University of Connecticut, Storrs, USA. He was the Francis L. Castleman Distinguished Professor at the University of Connecticut during 2017-2018. He was a System Planning Engineer at BC Hydro and Power Authority, Vancouver, during 2006-2010. His research interests include microgrids, cyber security, power system stability and control, and smart ocean systems.

Dr. Zhang is an individual member of CIGRÉ. He is an Editor for the IEEE Transactions on Power Systems, the IEEE Transactions on Sustainable Energy and the IEEE Power and Energy Society Letters, an Associate Editor for the IEEE Journal of Oceanic Engineering and the IEEE Transactions on Industrial Electronics.

Chongqing Kang (M'01−SM'07−F'17) received the Ph.D. degree from the Department of Electrical Engineering in Tsinghua University, Beijing, China, in 1997.

He is currently a Professor in Tsinghua University. His research interests include power system planning, power system operation, renewable energy, low carbon electricity technology and load forecasting.